AGU PUBLICATIONS

JGR

Journal of Geophysical Research: Space Physics

RESEARCH ARTICLE
10.1002/2014JA019864

Key Points:
- Test particle simulations of the loss of inner belt protons by mu scattering
- Analytic models assuming fixed cutoff conditions may overpredict the loss
- A new "epsilon-onset" model to predict the proton loss due to mu scattering

Correspondence to:
W. Tu,
wtu@lanl.gov

Citation:
Tu, W., M. M. Cowee, and K. Liu (2014), Modeling the loss of inner belt protons by magnetic field line curvature scattering, *J. Geophys. Res. Space Physics*, *119*, 5638–5650, doi:10.1002/2014JA019864.

Received 6 FEB 2014
Accepted 9 JUL 2014
Accepted article online 12 JUL 2014
Published online 25 JUL 2014

Modeling the loss of inner belt protons by magnetic field line curvature scattering

Weichao Tu[1], M. M. Cowee[1], and K. Liu[2]

[1]Space Science and Applications Group, Los Alamos National Laboratory, Los Alamos, New Mexico, USA, [2]Physics Department, Auburn University, Auburn, Alabama, USA

Abstract The sudden loss of energetic protons in the inner radiation belt has been observed during geomagnetic storms. It is hypothesized that this sudden loss occurs because of changes in the geomagnetic field configuration which lead to a breakdown of the first adiabatic invariant, μ, in a process called magnetic field line curvature scattering or μ scattering. Comparison of observations to various analytic model predictions for μ scattering induced loss has, however, yielded discrepancies. To better understand how well the analytic models predict the proton loss, test particle simulations are carried out for various magnetic field configurations. Although our simulation results agree well with the analytic models for single μ-scattering events, the results after cumulative μ scattering can show significant disagreement with the theoretical predictions based on analytic models. In particular, we find the assumption that protons with predicted initial $\delta\mu/\mu > 0.01$ or $\varepsilon > 0.1$ are ultimately lost overestimates the proton loss. Based on the test particle simulation results, we develop a new empirical model, called the "ε-onset" model, to predict the minimum value of ε at which all protons of a given pitch angle and energy can be assumed to be lost due to μ scattering. By applying our ε-onset model as the variable cutoff condition between trapping and detrapping, we obtain very good agreement between theoretical predictions and the simulation results for a range of *Kp*, suggesting that the ε-onset model can potentially serve as an easy-to-use and more reliable predictor of inner belt proton loss due to μ scattering than the previously used fixed-valued cutoff conditions.

1. Introduction

Recent observations have shown that energetic protons (greater than tens of MeV) in the Earth's inner radiation belt ($L < 4$) can suddenly become detrapped and lost on timescales of hours during geomagnetic storms [*Selesnick et al.*, 2010; *Zou et al.*, 2011; *Looper et al.*, 2005; *Lorentzen et al.*, 2002]. Since these energetic protons can pose a significant hazard to space systems, understanding their dynamics is of great importance both scientifically and practically. It is thought that the detrapping of energetic protons is a consequence of changes in the trajectories of these large gyroradii protons due to the perturbed geomagnetic field [*Hudson et al.*, 1997; *Young et al.*, 2008; *Selesnick et al.*, 2010]. When the gyroradius (ρ_{gyro}) of a proton becomes large compared to the radius of curvature (R_c) of the magnetic field line or the distance traveled by a proton along the field line during one gyroperiod is comparable to R_c, the magnetic field experienced by the proton changes significantly during one gyroorbit and constants of motion cannot be determined (e.g., breaking the first adiabatic invariant, μ). The proton then exhibits chaotic behavior and will not be trapped. This process is referred to as magnetic field line curvature scattering, or μ scattering. As an example, the trajectories of a 50 MeV proton and a 500 MeV proton in a dipole magnetic field are shown in Figure 1, with the 50 MeV proton exhibiting adiabatic bounce and drift motion (Figure 1a, with $\rho_{gyro} \ll R_c$ at equator), and the 500 MeV proton exhibiting nonadiabatic motion (Figure 1b, with $\rho_{gyro} \sim R_c$).

There are a number of analytic models which predict the μ scattering of a given proton on a given magnetic field line based on parameters calculated from the proton's energy (E) and equatorial pitch angle (α_{eq}), and the local magnetic field properties. A commonly used parameter is ε (also known as κ, where $\kappa = \sqrt{1/\varepsilon}$), equal to $\rho_{gyro}(\alpha_{eq} = 90^o)/R_c$ (equator), where $\rho_{gyro}(\alpha_{eq} = 90^o)$ is the gyroradius of a $\alpha_{eq} = 90°$ proton and R_c (equator) is the radius of curvature of the magnetic field line at the equator (the minimum curvature region) [*Speiser*, 1965; *West et al.*, 1978]. Nonadiabatic motion of particles occurs when ε is greater than or comparable to 1 (e.g., Figure 1b). A variety of analytic models have been derived to predict the change in μ during a single μ-scattering event; the quantity $\delta\mu/\mu$ is then defined as the relative change of μ during a single traversal

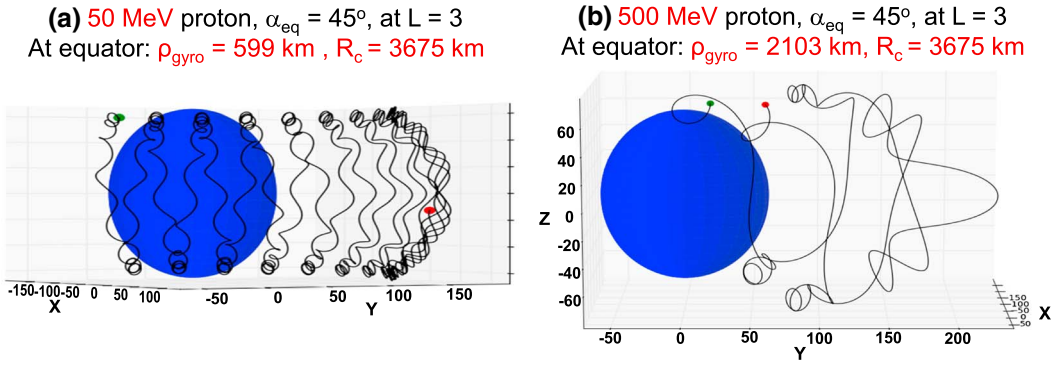

Figure 1. Trajectories of (a) a 50 MeV and (b) a 500 MeV proton initialized with $\alpha_{eq} = 45°$ at $L = 3$ traced in a dipole magnetic field (starting from the green point and ending at the red point). The 50 MeV proton exhibits adiabatic bounce and drift motion (Figure 1a, with $\rho_{gyro} \ll R_c$ at equator), while the 500 MeV proton exhibits nonadiabatic motion (Figure 1b, with $\rho_{gyro} \sim R_c$).

of the equator between two consecutive mirror points [*Birmingham*, 1984; *Il'in and Il'ina*, 1978; *Il'in et al.*, 1997; *Delcourt et al.*, 1996; *Young et al.*, 2002]. The $\delta\mu/\mu$ is shown to have a sinusoidal dependence on the proton's equatorial gyrophase, ψ_{eq}, with maxima in $|\delta\mu/\mu|$ at $\psi_{eq} = 0°$ (pointing toward the Earth) and $\psi_{eq} = 180°$ (pointing away from the Earth), where the curvature of the magnetic field line experienced by the proton as it crosses the equator is the largest. Since ψ_{eq} cannot be accurately determined in spacecraft observations, in order to apply these analytic models to predict the magnitude of μ scattering for a given proton, recent work has used the amplitude of the sinusoidal curve of $\delta\mu/\mu$ over all gyrophases [e.g., *Selesnick et al.*, 2010]. Thus, all protons on a given field line with a given E and α_{eq} are assumed to experience the maximum magnitude of μ scattering, regardless of their gyrophase. Then, in order to predict the loss of protons from cumulative μ-scattering events, it is assumed, based on previous analytic/empirical model studies, that the calculated ε or the $\delta\mu/\mu$ for the first μ-scattering event can be used as a predictor of the eventual fate of the proton. Typically, the conditions $\varepsilon > 0.1$ for small α_{eq} protons [*Sergeev and Tsyganenko*, 1982; *Young et al.*, 2008; *Zou et al.*, 2011] and $\delta\mu/\mu > 0.01$ [*Anderson et al.*, 1997; *Selesnick et al.*, 2010] are considered to represent the onset of nonadiabatic motion and eventually correspond to significant cumulative μ scattering ($\Delta\mu/\mu \sim 1$), resulting in detrapping and loss. Here we refer to $\varepsilon > 0.1$ and $\delta\mu/\mu > 0.01$ as cutoff conditions because they have been recently applied as such [*Selesnick et al.*, 2010; *Zou et al.*, 2011]; rather than being used to indicate the onset (i.e., the possibility) of loss, they are used to denote absolute loss. We also refer to $\varepsilon > 0.1$ and $\delta\mu/\mu > 0.01$ as "fixed-value" cutoffs because, even though the calculation of ε or $\delta\mu/\mu$ in the analytic model depends on the proton's pitch angle and energy and magnetic field configuration, the cutoff values of 0.1 and 0.01 have often been applied uniformly.

Comparison of the theoretical predictions of cumulative μ scattering which assume gyrophase independence and fixed-valued cutoffs to observations of the sudden loss of inner belt protons have yielded discrepancies. Looking at HEO data, *Selesnick et al.* [2010] reported that the sudden loss of 8–45 MeV protons at $L \sim 2$–3 occurred over a larger L range and exhibited a much more gradual decrease in L than predicted by their application of the *Birmingham* [1984] μ-scattering model, while the maximum L at which trapped protons were observed is consistent with μ-scattering theory. *Selesnick et al.* [2010] hypothesized that mechanisms other than μ scattering may also be acting on the minimum L side of the inner proton belt to produce losses whose energy dependence does not agree with the μ-scattering theory. Looking at POES data, *Zou et al.* [2011] reported that the loss of 70–500 MeV protons at $L \sim 1.5$–2.5 was generally consistent with the L range predicted by μ-scattering theory using the ε-based cutoff but that the agreement was not good for 35–70 MeV protons. Understanding the source of discrepancy between observations and these recent theoretical predictions of μ scattering based on analytic models motivates our study.

Most previous numerical simulations of μ scattering of particles focused on the change in μ during one equator crossing (i.e., single μ scattering) and focused on particles with a limited range of E, α_{eq}, and L [e.g., *Taylor and Hastie*, 1971; *Gray and Lee*, 1982; *Young et al.*, 2002]. *Anderson et al.* [1997] considered cumulative μ scattering over one drift orbit, but they mostly focused on protons with energies ≤1 MeV. Here we perform

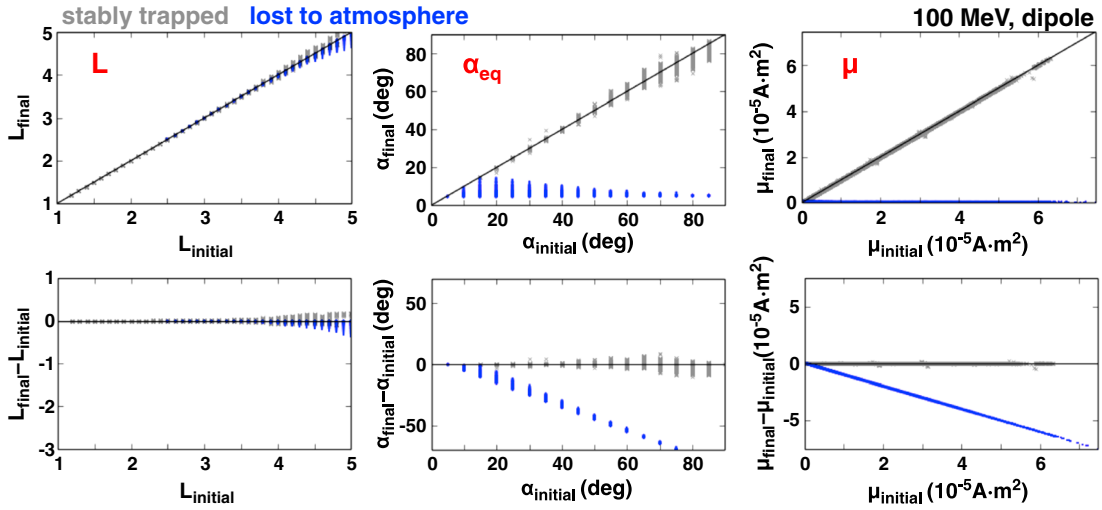

Figure 2. Plots of the simulated scattering behavior of the 100 MeV test protons in a dipole magnetic field. (top row) Scatter plots of the initial versus final L, α_{eq}, and μ for protons that end up being stably trapped (grey) or lost to the atmosphere (blue). (bottom row) The changes in L, α_{eq}, and μ versus the initial values. The stably trapped protons are traced for at least 15 drift orbits, and the untrapped protons are mostly lost to the atmosphere within 50 drift periods.

the first test particle simulations of cumulative μ-scattering events over tens to hundreds of drift periods for a large range of L, E, and α_{eq}, in order to better characterize the overall trapping and detrapping of a hypothetical proton population. The goals of this work are twofold: first, to investigate the possibility that the discrepancy between the observations and recent theoretical predictions is due to the assumptions of gyrophase independence and fixed-valued cutoffs for detrapping for all energies and equatorial pitch angles; second, to develop a new predictive model of detrapping due to μ scattering based on the test particle simulation results. Our methodology is introduced in section 2, with test particle simulation results and comparison with analytic model predictions shown in sections 3 and 4 for single and cumulative μ-scattering events, respectively. In section 4, we also introduce the "ε-onset" model, our new model that is empirically determined from simulations to predict the loss of inner belt protons under different magnetic field configurations. Final discussions and conclusions are presented in section 5.

2. Methodology: Test Particle Simulations

To study μ scattering of energetic protons in the inner radiation belt, we carry out test particle simulations which follow the full gyromotion of protons in a static background magnetic field. To isolate effects due to magnetic field line curvature scattering of the energetic protons, we do not include electric fields in the simulation. Protons are iterated in time using a relativistic fourth-order Runge-Kutta solver [*Press et al.*, 2007] with an adaptive time step (20–40 steps per gyroperiod). The simulation code has been tested for accuracy by carrying out a series of runs for adiabatic protons, to verify that the orbital paths and the gyro/bounce/drift periods are correct and unchanging over hundreds of drift periods. The proton energies are also verified to be nearly perfectly conserved during the simulations (energy changes by 0.00027% over 10 drift orbits).

Protons are initialized uniformly in L ($L = 1$–5, $\Delta L = 0.1$), equatorial pitch angle ($\alpha_{eq} = 5°$–$85°$, $\Delta\alpha_{eq} = 5°$), at various energies ($E = 25$, 50, 100, 200 MeV), and are launched from their mirror points at midnight local time. We do not launch $\alpha_{eq} = 90°$ protons because exactly 90° particles do not μ scatter, due to the fact that they do not see parallel gradients in the magnetic field [*Anderson et al.*, 1997]. Because μ scattering is gyrophase dependent, we launch a set of protons that is uniformly spaced in gyrophase ($\psi_{eq} = 0° \sim 360°$, $\Delta\psi_{eq} = 6°$) for each E, α_{eq}, and L combination. Therefore, we trace ~171,000 protons under each field configuration, including a pure dipole magnetic field and the T89c magnetic field model [*Tsyganenko*, 1989] with an internal dipole field at $Kp = 0$–6. This number of test particles was chosen to permit sufficient statistical sampling while minimizing the run time.

Energetic protons are traced in the simulation until they are either lost or stably trapped. Protons are considered lost if they exit the simulation box (radial distance $>$ 15 Earth radius) or if they enter the

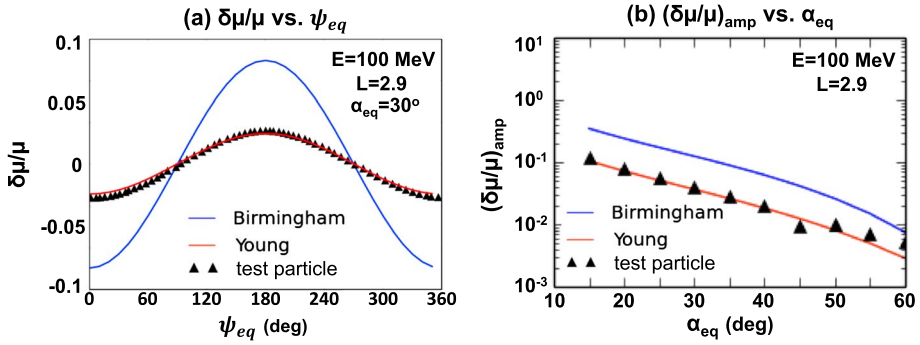

Figure 3. Comparison between the test particle simulation results (black triangles) and analytic model predictions (*Birmingham* [1984] model in blue, *Young et al.* [2002] model in red) for $\delta\mu/\mu$ during single μ-scattering events, with (a) the gyrophase dependence and (b) the α_{eq} dependence.

atmosphere (altitude $<$ 1000 km to mimic loss into the drift loss cone assuming having an offset-tilted dipole; protons mirroring above 1000 km at any longitude are guaranteed to mirror above 100 km, which is the atmosphere height, at South Atlantic Anomaly under the International Geomagnetic Reference Field model). Protons whose mirror point magnetic field strength changes $<$0.5% over 15 consecutive drift orbits are considered stably trapped. The value of μ is calculated as the first-order term only, such that $\mu \sim \mu_0 = p_\perp^2/(2m_0B)$, where $p_\perp$ is the proton's relativistic momentum perpendicular to the magnetic field direction and m_0 is its rest mass. We only calculate μ at the mirror points using the B field at the average gyrocenter, so that higher-order μ terms are minimized [*Anderson et al.*, 1997; *Young et al.*, 2002]. However, the extra accuracy obtained by calculating μ at the gyrocenter mirror points breaks down at large equatorial pitch angles (not valid for $\alpha_{eq} > 60°$) [see *Young et al.*, 2002, Appendix A2]. Values of α_{eq} and L for the tested protons are also calculated from the average gyrocenter.

We start by tracing 100 MeV protons in a dipole field. Figure 2 (top) shows scatter plots of the initial versus final L, α_{eq}, and μ for protons that end up stably trapped (grey) or lost to the atmosphere (blue). In this run, no particles are lost outside the box. Figure 2 (bottom) shows the changes in L, α_{eq}, and μ versus the initial values. Note that in Figure 2 (top right) the protons with $\mu_{final} = 0$ are lost into the atmosphere (inner boundary at 1000 km). The black line shows $x = y$ in the top row and zero in the bottom row. The simulation results show that the stably trapped protons generally conserve their L, α_{eq}, and μ, while the protons that are lost to the atmosphere have been scattered to smaller α_{eq} and μ (middle and right columns). Protons which are eventually lost could have started with any α_{eq} ($<$90°), indicating that the cumulative changes in pitch angle can be large.

3. Simulation Results: Single μ-Scattering Events

One goal of our study is to compare the test particle simulation results with predictions from analytic models. First, we will compare the change in μ during single μ-scattering events. Since the analytic models were originally derived based on single μ-scattering events, we expect the analytic model predictions to agree reasonably well with our simulation results. For the run tracing 100 MeV protons under a dipole, Figure 3 shows $\delta\mu/\mu$ during a single traversal of the equator from mirror point to mirror point, versus gyrophase ψ_{eq} in Figure 3a and versus equatorial pitch angle α_{eq} in Figure 3b (not over the entire range of α_{eq} since the μ calculation at the gyrocenter mirror points is not accurate for $\alpha_{eq} > 60°$ [*Young et al.*, 2002]). Note the $\delta\mu/\mu$ in Figure 3a is the definition of $\delta\mu/\mu$ with the gyrophase dependence, while the $\delta\mu/\mu$ in Figure 3b is the amplitude of the sinusoidal curve in Figure 3a over all gyrophases (as discussed in section 1). In Figure 3, the blue curve is the predicted $\delta\mu/\mu$ using the Birmingham model given by the following:

$$\frac{\delta\mu}{\mu} = -\frac{\pi}{2^{1/4}\Gamma(9/8)}\frac{1}{\varepsilon^{1/8}\sin\alpha_{eq}}\exp\left(-\frac{F(\sin\alpha_{eq})}{\varepsilon}\right)\cos\psi_{eq} \quad (1)$$

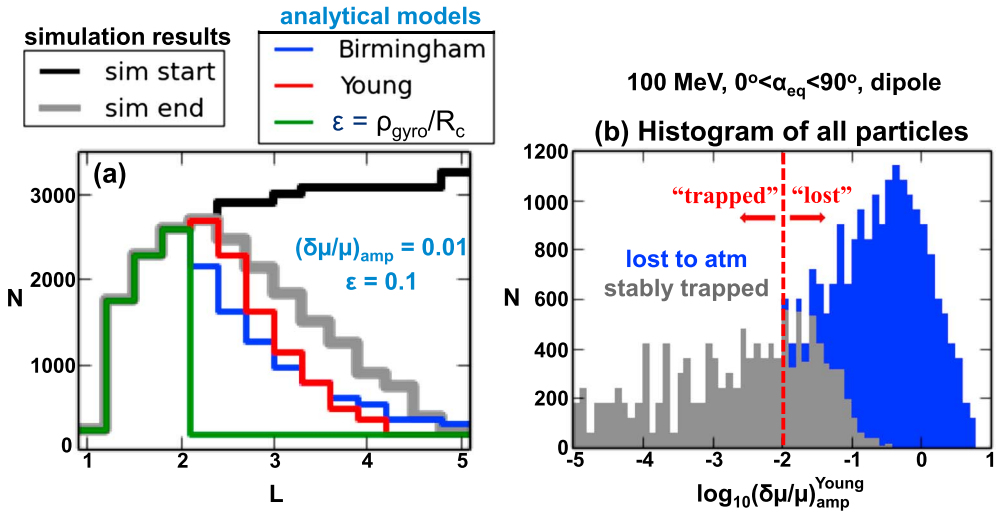

Figure 4. (a) Comparison between the simulation results and theoretical predictions for the trapped proton distribution in a dipole field versus *L* (with *L* bin size of 0.3). Shown is the test proton distribution at the beginning (black) and end (grey) of the simulation, compared with theoretical predictions based on analytic models (green for ε, blue for *Birmingham* [1984] model, and red for *Young et al.* [2002] model) assuming fixed-valued cutoff conditions. (b) Histogram of all test protons in the 100 MeV dipole run, plotted versus the $\delta\mu/\mu$ predicted by the Young model. Blue indicates protons lost into the atmosphere, and grey indicates stably trapped protons. The red dashed line indicates the fixed cutoff value of $\delta\mu/\mu = 0.01$.

Equation (1) is reconstructed from equation (21) in *Birmingham* [1984] (or *Anderson et al.* [1997, equations (8) and (9)]) with the functional form of *F* given by equation (10) in *Anderson et al.* [1997]. The red curve in Figure 3 is the predicted $\delta\mu/\mu$ using the Young model, which is given by the following:

$$\frac{\delta\mu}{\mu} = \frac{2}{\sin^2\alpha_{eq}}\left[F(\varepsilon,\alpha_{eq}) + A(\varepsilon,\alpha_{eq})\cos\psi_{eq}\right] \quad (2)$$

Equation (2) is reconstructed from equations (5) and (6) in *Young et al.* [2002], with the functional forms of $F(\varepsilon,\alpha_{eq})$ and $A(\varepsilon,\alpha_{eq})$ given by equations (15a) and (15b) in *Young et al.* [2002], respectively. Both the $\delta\mu/\mu$ from the Birmingham and the Young models vary with proton's equatorial pitch angle (α_{eq}), energy (since ε depends on proton energy), and gyrophase. These two models are chosen because the Birmingham model is commonly used (relatively easy to implement) and the Young model has been shown to be the most accurate of the existing models for an arbitrary magnetic field. The black triangles in Figure 3 are $\delta\mu/\mu$ calculated from our test particle simulation. We find that the *Young et al.* [2002] model performs very well in predicting both the gyrophase and equatorial pitch angle dependence of $\delta\mu/\mu$, while the *Birmingham* [1984] model overestimates the amplitude of $\delta\mu/\mu$ for this case. This is not surprising since the Young model is derived and tested with a very accurate orbit integration scheme [*Young et al.*, 2002]. They also suggested that the *Birmingham* [1984] model is not as accurate, which is partially attributed to the fact that it was derived for a magnetotail-like configuration. The agreement between our test particle simulation results and the Young model predictions for single μ-scattering events further validates our test particle simulation code.

4. Simulation Results: Cumulative μ-Scattering Events

4.1. Comparison With Analytic Model Predictions

Next, we investigate cumulative μ-scattering effects and compare the simulated loss of protons induced by magnetic field line curvature scattering with theoretical predictions based on analytic models when gyrophase independence and fixed-valued cutoffs are assumed. For the run with 100 MeV protons under a dipole as discussed in the previous section, the proton distribution summed over all the gyrophases and α_{eq} is plotted as a function of *L* in Figure 4a, with the black curve showing the initial proton distribution and the grey curve showing the remaining trapped particles by the end of simulation. We note that the initial distribution would be flat across *L* (since the simulation is initialized with uniform *L* loading), but to better visualize the loss due to μ scattering, we have subtracted the protons that are already inside the bounce loss

cone at the start of the simulation ($t = 0$). Comparing the initial to final distributions (black and grey curves), we see that protons at $L >$ ~2 can be lost into the atmosphere and we note that the majority of these are lost within ~50 drift periods (<1 h).

How does this μ-scattering loss modeled by our simulation compare with theoretical predictions based on analytic models? As discussed in section 1, fixed cutoff values for trapping and detrapping, $\delta\mu/\mu = 0.01$ or $\varepsilon = 0.1$, are applied to the analytic models to obtain the loss predictions. Even though the cutoff of $\varepsilon = 0.1$ is generally applied to protons with small equatorial pitch angles [*Selesnick et al.*, 2010; *Zou et al.*, 2011], here to distinguish it from the $\delta\mu/\mu = 0.01$ cutoff, it is applied to protons at all pitch angles (with $\alpha_{eq} = 5°$–$85°$) for demonstration purpose. Taking the *Selesnick et al.* [2010] application of the *Birmingham* [1984] model as an example, $\delta\mu/\mu$ for each proton is calculated from its initial L, α_{eq}, and energy, and it is assumed that $\psi_{eq} = 0°$ for all particles. The protons with $\delta\mu/\mu \geq 0.01$ are then predicted to be lost into the atmosphere. The predicted distribution of trapped protons (i.e., $\delta\mu/\mu < 0.01$) is given by the blue curve in Figure 4a. Applying a similar procedure for the *Young et al.* [2002] (equation (2) with $\psi_{eq} = 0°$ to remove the gyrophase dependence) and ε models, the predicted distributions of trapped protons are shown by the red and green curves, respectively. The comparison between the simulation results and these theoretical predictions shows that they all overpredict the loss of inner belt protons due to μ scattering, with the poorest performance from the ε model. Similar to the conclusions in *Selesnick et al.* [2010], the maximum L of the stably trapped protons in the test particle simulations (the grey curve extends to $L_{max} \sim 5$) is generally consistent with the prediction based on the *Birmingham* [1984] model (blue curve extends to similar L_{max} location); however, poor agreement is found with the gradient of the trapped proton distribution in L.

We have demonstrated the theoretical predictions based on analytic models, but assuming gyrophase independence and fixed-valued cutoff conditions can significantly overpredict the μ-scattering loss of inner belt protons, even though the analytic models themselves include dependences of the magnetic field model and the proton's pitch angle and energy. Results in section 3 have already demonstrated that the *Young et al.* [2002] model fairly well predicts the $\delta\mu/\mu$ during single μ-scattering events. Thus, the poor performance in predicting cumulative μ scattering of protons is likely due to the assumptions made in the theoretical predictions, such as the fixed-valued cutoff conditions for detrapping applied to all protons. To investigate this, a histogram of all protons in the 100 MeV dipole run is plotted in Figure 4b versus the logarithm of $\delta\mu/\mu$ (the amplitude without gyrophase dependence) predicted by the *Young et al.* [2002] model for the first-half bounce (single scattering). Blue areas indicate protons that are eventually lost to the atmosphere in the simulation, and the grey areas indicate stably trapped protons. The histogram shows that there is no clear cutoff in $\delta\mu/\mu$ between the trapped and lost protons. If a fixed-valued cutoff of $\delta\mu/\mu = 0.01$ is assumed (as for Figure 4a), protons on the right-hand side of the vertical line in Figure 4b (red dashed line at $\delta\mu/\mu = 0.01$) will be predicted as lost, while protons on the left-hand side will be predicted as trapped. Therefore, a fair amount of trapped protons in the simulation (grey areas on the right-hand side of the red dashed line) will be predicted as lost using the fixed-valued cutoff condition, leading to overprediction of the loss from these applications of the analytic models. While these results explain the overprediction of loss, they do not provide a physical explanation of why there is no fixed-valued cutoff in $\delta\mu/\mu$ between trapped and lost protons, given that the analytic models include a dependence on proton pitch angle and energy. This will be further investigated in the following two subsections.

4.2. Gyrophase Dependence of Trapping and Loss

As discussed in section 1, because the gyrophase cannot be accurately determined in observations, in order to apply analytic models to predict the μ-scattering induced loss of protons, gyrophase independence of $\delta\mu/\mu$ is assumed (i.e., assume $\psi_{eq} = 0°$). However, is cumulative μ scattering really gyrophase independent? To address this, we look more closely at our simulation results. The bar plot in Figure 5a illustrates the trapping and loss statistics from our simulation as a function of the proton's initial L for 100 MeV protons with initial $\alpha_{eq} = 30°$. The vertical axis is the number of protons (i.e., 60) launched in each E, L, α_{eq} bin, with black bars indicating the protons that are already inside the bounce loss cone at the start of the simulation, blue bars indicating protons that are lost into the atmosphere, and grey bars indicating protons that are stably trapped. The protons within each column are initialized at the same L, E, and α_{eq}, but they are started at different gyrophases (uniformly distributed in ψ_{eq}). Taking the column boxed in red as an example, the 60 protons are all initialized at $L = 2.9$ with $\alpha_{eq} = 30°$. The simulation results show that some protons end up lost into the

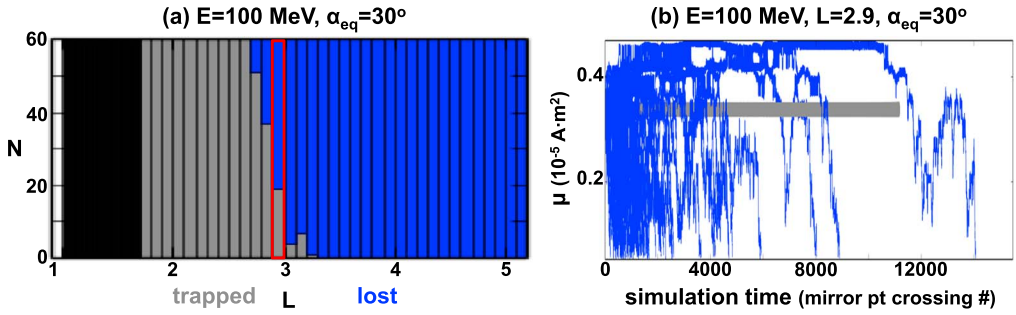

Figure 5. (a) Bar plot illustrating the trapping/loss statistics as a function of L from our simulation of 100 MeV, $\alpha_{eq} = 30°$ protons. The vertical axis is the number of protons, with black indicating protons that are already inside bounce loss cone at the start of the simulation, blue indicating protons that ended up lost into the atmosphere, and grey indicating protons that ended up stably trapped. (b) Graph showing μ versus time for the 60 protons indicated by the red box in Figure 5a, with the trapped protons plotted with grey lines and the protons lost to atmosphere plotted with blue lines.

atmosphere while others are stably trapped, depending on their gyrophases. The time history of μ for these 60 protons is shown in Figure 5b. Again, the stably trapped protons keep a relatively constant μ (grey lines), but others suffer from μ scattering and are eventually lost into the atmosphere (i.e., μ goes to zero) at different times through the simulation (blue curves). Therefore, the simulation results demonstrate that, similar to single μ-scattering events, the final state after cumulative μ-scattering events is also gyrophase dependent. This is consistent with the findings in *Anderson et al.* [1997] where test particles are traced for one complete drift. Due to this gyrophase dependence, there is no cutoff in L between trapped (grey) and lost (blue) protons in Figure 5a, leading to no cutoff in $\delta\mu/\mu$ between trapped and lost protons at specific proton energy and α_{eq}. However, this gyrophase dependence of cumulative μ scattering is very unpredictable due to the phase randomness of the scattering process after tens to hundreds of bounce and drift motion of energetic protons. Accordingly, as shown in Figure 5a, whether a proton is trapped or lost does not exhibit a regular pattern between $L = 2.7$ and 3.3.

4.3. Variable Loss Onset

Given that the results show that there is a gyrophase dependence of μ-scattering induced loss, but the gyrophase angle cannot be accurately determined by spacecraft observations, we must examine quantities that are associated with this gyrophase dependence but are more observable; for example, the "loss onset." The L of the onset of loss due to μ scattering, defined as L_{onset}, is the L value above which the loss of protons starts to occur. L_{onset} is marked as red vertical lines in Figures 6a1–6a3 for 100 MeV protons initialized at different equatorial pitch angles ($\alpha_{eq} = 30°$, 40°, and 50°, respectively). The format of the bar plot in Figures 6a1–6a3 is the same with Figure 5a (with Figure 6a1 identical to Figure 5a). The simulation results show that L_{onset} increases as α_{eq} increases, from $L_{onset} = 2.7$ at $\alpha_{eq} = 30°$ to $L_{onset} = 3.4$ at $\alpha_{eq} = 50°$. The variation of L_{onset} over the full α_{eq} range is plotted in Figure 6b, as determined from simulations of 100 MeV protons in a dipole with 14 different initial α_{eq} values (outside the bounce loss cone). Even though L_{onset} does not perfectly increase with α_{eq} (e.g., at $\alpha_{eq} = 60°$ and 75°, caused by statistical fluctuations possibly due to limited L resolution and number of particles in the simulation), we note that L_{onset} exhibits a predictable pattern versus α_{eq}, indicating that the loss onset could be a predictable quantity. Now the question is as follows: how useful is the loss onset in the prediction of proton loss due to μ scattering? For the simulation of 100 MeV protons in a dipole, if we ignore the gyrophase dependence and use the α_{eq}-dependent loss onset as an explicit cutoff (rather than an onset threshold) between the trapped and lost protons such that the protons with $L < L_{onset}$ (excluding the protons in black bars) will be predicted as trapped and the protons with $L \geq L_{onset}$ will be predicted as lost, then only a small number of trapped protons in the simulation will be mispredicted as lost. If this assumption is applied to all the equatorial pitch angles, the prediction of the stably trapped protons will be the grey distribution shown in Figure 6c. The histogram in Figure 6c includes four different proton populations including those inside the bounce loss cone at the start of the simulation (black), those that are stably trapped (grey) or lost (blue) in the simulation which were correctly predicted as "'trapped" or "lost" using the loss onset as the cutoff, and those that are stably trapped in the simulation but

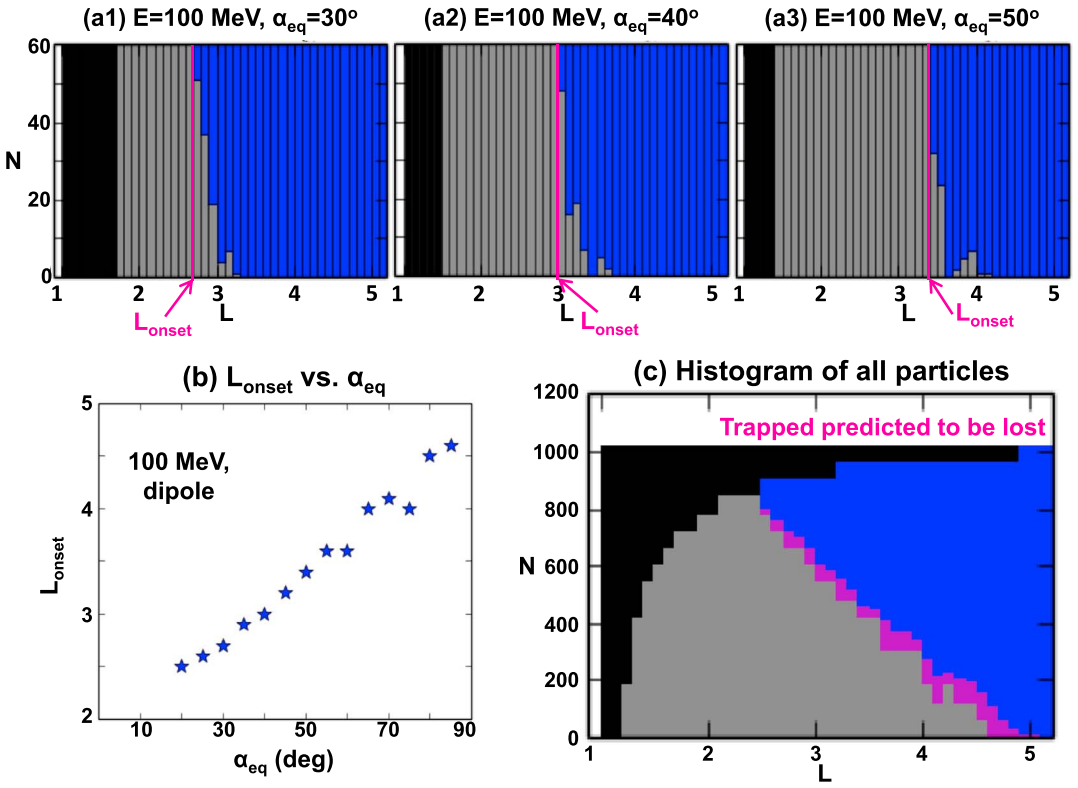

Figure 6. (a1–a3) Bar plots with the same configuration as Figure 5a but initialized at different α_{eq}, with the red vertical lines marking L_{onset} locations. (b) L_{onset} versus α_{eq} for the 100 MeV, dipole run. (c) Histogram of the 100 MeV protons in a dipole as a function of L (similar to Figure 4a but with L bin size of 0.1), including protons (black) inside loss cone at the start of the simulation, stably trapped and predicted as "trapped" by using loss onset as the cutoff (grey), protons lost into the atmosphere and predicted as lost (blue), and trapped but mispredicted as lost (magenta).

mispredicted as lost using the loss onset as the cutoff (magenta). This shows that, if a variable loss onset, which depends on E and α_{eq}, is used as the cutoff between trapped and lost protons, then the predicted loss includes the protons in both the blue and magenta areas. Even though this still somewhat overpredicts the loss (since the magenta protons are actually trapped), the overprediction is relatively small and the L gradient of trapped proton distribution is well preserved, which is an improvement from the previous theoretical predictions with fixed-valued cutoffs for all protons. Based on these results, we conclude that a more accurate μ-scattering induced loss prediction model can be developed by predicting the loss onset as a function of E and α_{eq} and using it as a variable cutoff between trapped and lost protons. The development of this new model is detailed in the next section.

4.4. New ε-Onset Model for Loss Prediction

Our test particle simulation results suggest that theoretical predictions for μ scattering based on analytic models will overpredict the loss if cutoff conditions for detrapping are taken as constant for all particles. On the other hand, we find that using the variable loss onset-based cutoff conditions makes a more accurate loss prediction. Here we investigate if the variable loss onset can be parameterized using the existing analytic models with which the community is already familiar (e.g., the $\delta\mu/\mu$ and ε models) and then be applied to predict the μ-scattering loss of inner belt protons.

Based on the L_{onset} versus α_{eq} distribution derived from the test particle simulations for 100 MeV protons under dipole (Figure 6b), we can calculate the corresponding $(\delta\mu/\mu)_{onset}$ and ε_{onset} using the analytic model equations [*Birmingham*, 1984; *Young et al.*, 2002]. Figure 7a shows the dependence of $(\delta\mu/\mu)_{onset}$ on α_{eq} based on the Birmingham model (left, using equation (1) without the gyrophase dependence) and Young model (right, using equation (2) without the gyrophase dependence) for 100 MeV protons under a dipole (note that

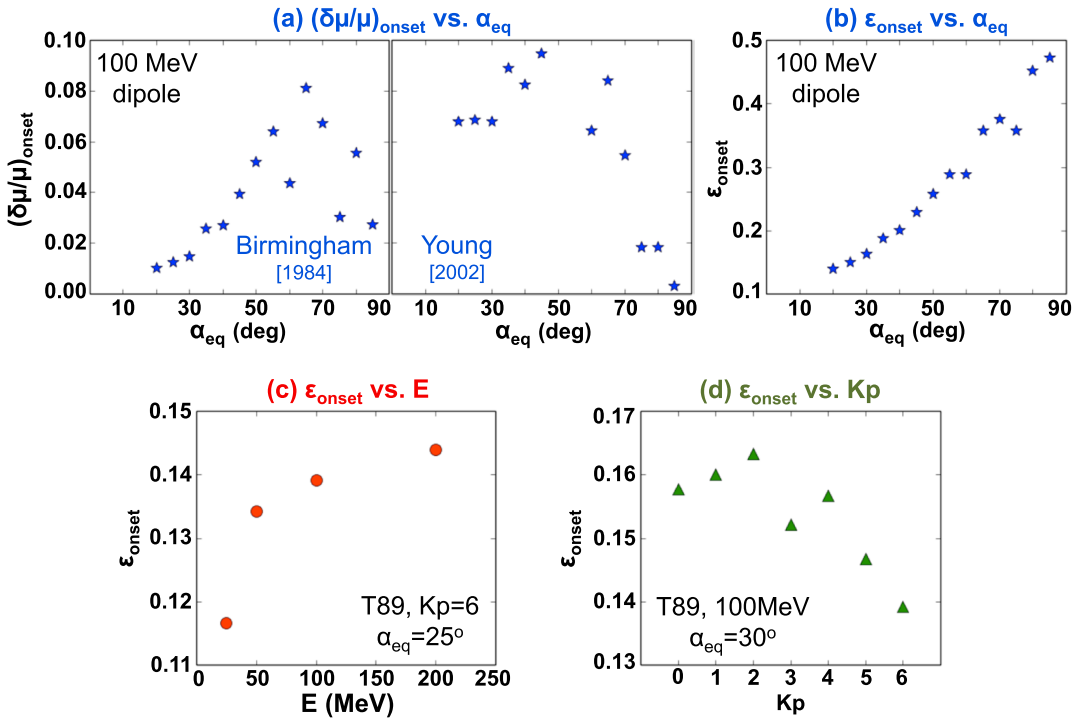

Figure 7. (a) Graph showing $(\delta\mu/\mu)_{\text{onset}}$ versus α_{eq} from the test particle simulation for 100 MeV protons under dipole calculated using the (left) *Birmingham* [1984] model and (right) *Young et al.* [2002] model. (b–d) Graph showing $\varepsilon_{\text{onset}}$ versus α_{eq}, *E*, *Kp*, respectively, calculated from a series of runs of the test particle simulations.

the Young model, though applied to all α_{eq} here, is only valid for $\alpha_{\text{eq}} < 60°$ since the μ calculation at the gyrocenter mirror points is not accurate for large α_{eq} [*Young et al.*, 2002]). The $\varepsilon_{\text{onset}}$ versus α_{eq} variation is shown in Figure 7b. The results show that the $(\delta\mu/\mu)_{\text{onset}}$ and $\varepsilon_{\text{onset}}$ calculated from the test particle simulations are not constant valued, with $(\delta\mu/\mu)_{\text{onset}}$ mostly above 0.01 and $\varepsilon_{\text{onset}}$ generally >0.1. This further indicates that if $\delta\mu/\mu = 0.01$ or $\varepsilon = 0.1$ is assumed as a constant cutoff between trapping and loss, as has been generally assumed in the literature, the μ-scattering induced loss will be overpredicted. Comparing the α_{eq} dependence of the loss onset expressed in the three different analytic models (*Birmingham* [1984], *Young et al.* [2002], and ε), we find that $\varepsilon_{\text{onset}}$ is most suitable to parameterize the loss onset, because its dependence on α_{eq} exhibits a clear pattern compared to the other two models. Specifically, $\varepsilon_{\text{onset}}$ is shown to decrease as α_{eq} decreases because first of all, μ-scattered particles starting off with small equatorial pitch angles that are closer to the loss cone have a greater chance of ending up in the loss cone than the ones with initially larger equatorial pitch angles; additionally, particles with small α_{eq} travel longer distance along the field line in one gyroperiod, thus having a greater chance of being lost when passing through the region of minimum field line curvature. Using ε is also beneficial because it is a well-known quantity that is easy to calculate. Thus, an ε-onset model will be developed here to provide the value of $\varepsilon_{\text{onset}}$ as a function of α_{eq}, proton energy, and magnetic field configuration.

With the α_{eq} dependence of $\varepsilon_{\text{onset}}$ at fixed energy and fixed field configuration shown in Figure 7b, examples of its dependence on proton energy and magnetic field configuration (expressed in *Kp* levels in T89c model) are shown in Figures 7c and 7d, respectively. These results are calculated from a series of test particle simulations for protons at four different energies, 18 different equatorial pitch angles, and in a dipole or T89c model magnetic field at different *Kp* levels (details described in section 2). Based on these results, an ε-onset model which provides the value of $\varepsilon_{\text{onset}}$ as a function of α_{eq}, proton energy *E*, and *Kp* is developed as expressed in the following equations:

$$\text{For a pure dipole}: \quad \varepsilon_{\text{onset}} = \left[A\exp\left(B\sin\alpha_{eq}\right) + C\right](E/E_0)^D \tag{3}$$

$$\text{For the T89c model at different } Kp: \quad \varepsilon_{\text{onset}} = \left[(a_0 + a_1 Kp)\exp\left(b\sin\alpha_{\text{eq}}\right) + c\right](E/E_0)^d \tag{4}$$

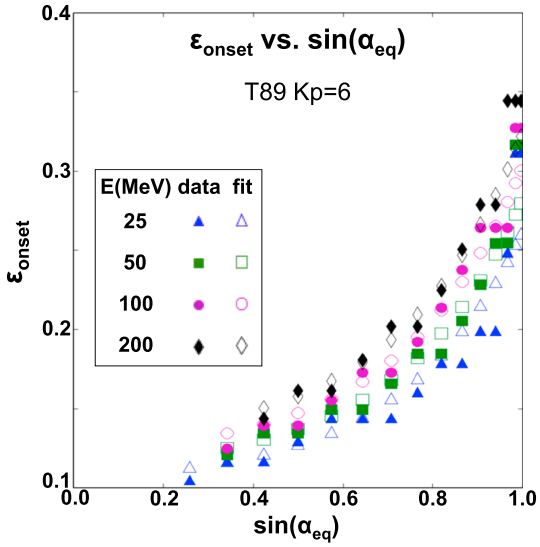

Figure 8. Graph showing ε_{onset} versus sin (α_{eq}) for protons at four different energies (different colors and symbols) at $Kp = 6$. Solid markers are ε_{onset} directly calculated from the test particle simulations, and the open markers are the fitted ε_{onset} values from the ε-onset model.

where $E_0 = 25$ MeV, free parameters include A, B, C, and D for dipole model, and a_0, a_1, b, c, and d for the T89c magnetic field model driven by Kp. The functional forms of equations (3) and (4) are chosen by investigating the α_{eq}, E, and Kp dependence of ε_{onset} (examples shown in Figures 7b–7d). Note that the ε_{onset} for a nondipole field is estimated at midnight local time where the magnetic field is the most stretched and where the maximum ε occurs. The free parameter values are determined by least squares fits of the model equations to the ε_{onset} values calculated from the test particle simulations, with the best fit values shown below:

$$\text{For dipole model}: \quad A = 0.011,\ B = 3.358,\ C = 0.1,\ D = 0.026$$

$$\text{For T89c model}: \quad a_0 = 5.2e-3,\ a_1 = -2.47e-4,\ b = 3.76,\ c = 0.1,\ d = 0.1$$

To illustrate the quality of the fit from the ε-onset model, in Figure 8 we plot the ε_{onset} directly calculated from the test particle simulations (solid markers) at $Kp = 6$ for protons at four different energies, as a function of sin (α_{eq}). Different colors and symbols represent different energies (see figure legend). The fitted ε_{onset} values from the ε-onset model (equation (4) for T89c) are also plotted (open markers). The results demonstrate that the ε-onset model well captures the variation of ε_{onset} versus α_{eq} and proton energy, with a Mean Absolute Percentage Error (MAPE) as low as 5.14% for the results in Figure 8 (MAPE is defined as $\text{MAPE}\,(\%) = \sum_{i=1}^{n}\left|\frac{m_i - d_i}{d_i}\right| \times 100/n$, where m_i is the fitted ε_{onset} value calculated from equation (4) at $Kp = 6$, d_i is the ε_{onset} value calculated from the test particle simulations, and n is the number of points in Figure 8 [*Tu et al.*, 2013]).

As discussed in section 4.3, using this newly developed ε-onset model in which the cutoff between trapped and lost protons varies with α_{eq}, proton energy E and Kp, we can better predict the loss of inner belt protons due to μ scattering. A prediction can be made by following these steps:

1. Identify proton's L, E, and α_{eq} (here we use the initial L, E, and α_{eq} values for protons in the test particle simulations).
2. Calculate the maximum ε for that proton on its drift shell (e.g., at midnight), defined as ε_{proton}.
3. Calculate ε_{onset} using the above equation (3) or (4) depending on the background field; if a nondipole field, take the maximum Kp value during the storm).
4. If $\varepsilon_{proton} \geq \varepsilon_{onset}$, the proton is predicted as lost; otherwise, it is predicted to be trapped.

Following the above procedure, the predictions of the μ-scattering induced loss based on the ε-onset model are shown in Figure 9 in comparison with the test particle simulation results. Similar to Figure 4a, in

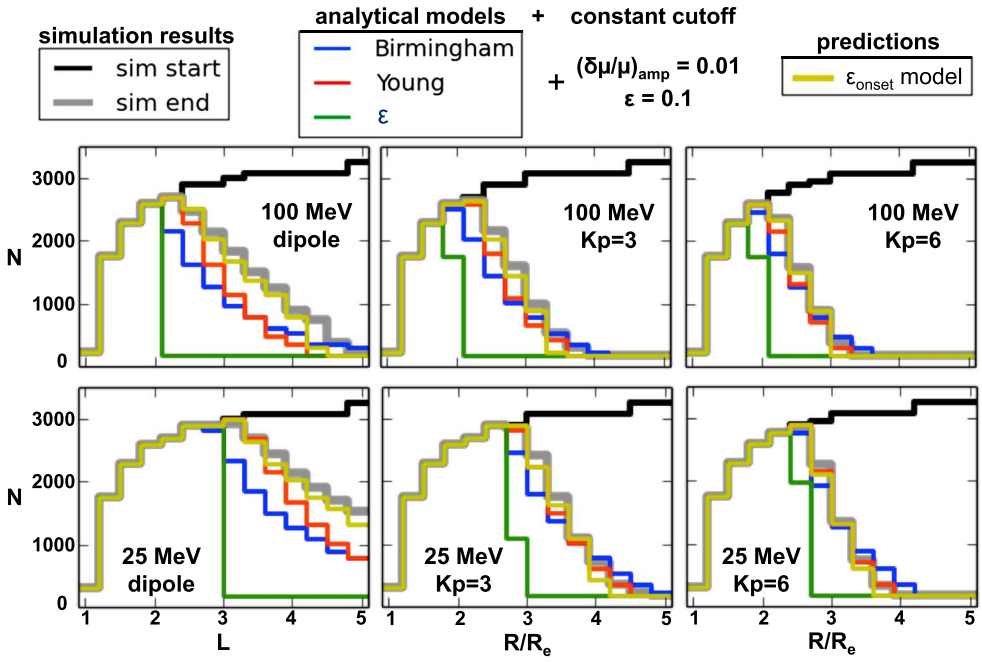

Figure 9. Comparison between the simulation results and theoretical predictions based on analytic models for the trapped proton distributions (each panel has the same configuration as Figure 4a but for varying proton energy and *Kp*). New predictions using the ε-onset model are plotted in yellow.

each panel of Figure 9, the proton distribution in the test particle simulation starts from the black curve and ends with the grey curve (the remaining stably trapped protons); the theoretical predictions using analytic models with fixed-valued cutoff conditions ($\delta\mu/\mu = 0.01$ or $\varepsilon = 0.1$) for trapping and detrapping are shown as blue, red, and green curves for the Birmingham, Young, and ε models, respectively. Figure 9 (top) shows results for the 100 MeV protons under the different field configurations of dipole, T89c with $Kp = 3$, and T89c with $Kp = 6$; Figure 9 (bottom) is for the 25 MeV protons. Even though the new ε-onset model has been tested for $Kp = 0$–6 (as covered by the T89c model), only the cases with $Kp = 3$ and 6 are shown here as examples. Comparing the simulation results to the theoretical predictions with fixed-valued cutoffs at different *Kp* levels, we find that using the fixed-valued cutoff at $\varepsilon = 0.1$ is always a very poor predictor of the loss, as was shown by *Young et al.* [2002] and *Anderson et al.* [1997]; while the *Birmingham* [1984] and the *Young et al.* [2002] models with fixed-valued cutoff at $\delta\mu/\mu = 0.01$ overpredict the loss but become more accurate as *Kp* increases. The prediction for stably trapped protons using the ε-onset model with its variable cutoff between trapped and lost protons is indicated by the yellow curve, and we find that this model well reproduces the μ-scattering induced loss of inner belt protons for a range of energies (25–200 MeV) and magnetic field models (dipole and T89c with $Kp = 0$–6). In particular, it reproduces the *L* gradient of the trapped proton distribution which is poorly predicted by previous analytic models for a dipole or for T89c with $Kp = 3$. The predictions from the ε-onset model do not perfectly agree with the test particle simulations for two reasons: first, the ε_{onset} equations, equations (3) and (4), do not perfectly fit the test particle simulation results (e.g., Figure 8); second, the ε-onset model is expected to slightly overpredict the loss since it ignores the gyrophase dependence of cumulative μ scattering (as illustrated in Figure 6c). Even though the performance of using our new ε-onset model and using the *Young et al.* [2002] model with fixed-valued cutoff condition is comparable for 25 MeV protons at $Kp = 6$ (Figure 9, bottom right), an advantage of using our ε-onset model over the *Young et al.* [2002] model is its ease to apply. The *Young et al.* [2002] model requires calculation of a larger number of field-related parameters, including first and second derivatives of *B* and R_c, than the ε-onset model. Furthermore, the consistently good performance of the ε-onset model over the range of proton energies, equatorial pitch angles, and magnetic field configurations tested demonstrates its general fidelity and potential usefulness in predicting the loss of inner belt protons due to μ scattering.

5. Conclusions and Discussions

In order to understand the loss of energetic protons in Earth's inner radiation belt due to magnetic field line curvature scattering, or μ scattering, test particle simulations have been carried out for different magnetic field conditions. Comparisons have been made between the simulation results and the theoretical predictions from analytic models for both single and cumulative μ-scattering events. Our test particle simulations suggest that analytic models can well reproduce the change in μ due to a single equator crossing (single μ-scattering event). For example, excellent agreement is reached between the simulation results and the *Young et al.* [2002] model predictions of $\delta\mu/\mu$ for single scatters as a function of gyrophase angle and equatorial pitch angle. However, the eventual detrapping and loss of inner belt protons due to cumulative μ scattering may be poorly predicted if gyrophase independence and fixed-valued cutoff conditions between trapping and detrapping are applied to the analytic models. Specifically, we find that the use of any analytic model (e.g., *Birmingham* [1984] or *Young et al.* [2002]) with the fixed-valued cutoff condition, $\delta\mu/\mu = 0.01$, can significantly overpredict the loss due to μ scattering under certain circumstances. This is due to the fact that μ scattering is gyrophase dependent and, more importantly, that the loss onset cannot be accurately predicted by a fixed value of ε (or $\delta\mu/\mu$), despite the fact that the analytic models depend on proton energy E, equatorial pitch angle α_{eq}, and magnetic field configuration. Instead, we find that the loss onset is better predicted by a value of ε that varies with E, α_{eq}, and magnetic field configuration. Based on the test particle simulation results, a new empirical model is developed to predict the loss of inner belt protons due to μ scattering, which we call the ε-onset model. The model is parameterized by E, α_{eq}, and Kp to yield a value of ε that can be used as a cutoff value for trapping or loss of protons. The ε-onset model is demonstrated to better predict the simulation results than the previous theoretical predictions based on applications of the analytic models, and it is simple enough that it can be easily implemented.

With the current results, direct comparisons cannot yet be made between our new predictions and the observations, since our results are still in numbers of particles per bin and are initialized with uniform loading in each E, α_{eq}, and L bin (may not be realistic). However, based on the conclusions in *Selesnick et al.* [2010], the new model has already shown promise for a better agreement with the observations, e.g., with less steep L gradient of the predicted trapped proton. In the future, we will validate the ε-onset model against observations by focusing on reproducing observational case studies [e.g., *Selesnick et al.*, 2010]. To do this, more realistic initial conditions for the proton populations in E, α_{eq}, and L (rather than the uniform loading considered here) will be considered, simulation results given in number of test particles per E, α_{eq}, L bin will be converted to proton flux, and a virtual spacecraft will be flown through our simulations for detailed comparison. With this future work, we hope to better understand μ-scattering induced loss in the inner proton belt and demonstrate the usefulness of our model in predicting this loss.

Acknowledgments

We gratefully acknowledge the support of the U.S. Department of Energy through the LANL Laboratory Directed Research and Development (LDRD) Program for this work.

Michael Liemohn thanks the reviewers for their assistance in evaluating this paper.

Reference

Anderson, B. J., R. B. Decker, N. P. Paschalidis, and T. Sarris (1997), Onset of nonadiabatic particle motion in the near-Earth magnetotail, *J. Geophys. Res.*, *102*, 17,553–17,569, doi:10.1029/97JA00798.

Birmingham, T. J. (1984), Pitch angle diffusion in the Jovian magnetodisc, *J. Geophys. Res.*, *89*(A5), 2699–2707, doi:10.1029/JA089iA05p02699.

Delcourt, D. C., J. A. Sauvaud, R. F. Martin Jr., and T. E. Moore (1996), On the nonadiabatic precipitation of ions from the near-Earth plasma sheet, *J. Geophys. Res.*, *101*(A8), 17,409–17,418, doi:10.1029/96JA01006.

Gray, P. C., and L. C. Lee (1982), Particle pitch-angle diffusion due to nonadiabatic effects in the plasma sheet, *J. Geophys. Res.*, *87*, 7445–7452, doi:10.1029/JA087iA09p07445.

Hudson, M. K., S. R. Elkington, J. G. Lyon, V. A. Marchenko, I. Roth, M. Temerin, J. B. Blake, M. S. Gussenhoven, and J. R. Wygant (1997), Simulations of proton radiation belt formation during storm sudden commencements, *J. Geophys. Res.*, *102*(A7), 14,087–14,102, doi:10.1029/97JA03995.

Il'in, V. D., and A. N. Il'ina (1978), Mechanism of nonadiabatic losses in a dipole trap, *J. Theor. Exp. Phys.*, *48*, 259–262.

Il'in, V. D., A. N. Il'ina, and B. Y. Yushkov (1997), Change in the magnetic moment of a charged proton in a dipole magnetic field, *Plasma Phys. Rep. (translated from Russian)*, *23*(5), 367–371.

Looper, M. D., J. B. Blake, and R. A. Mewaldt (2005), Response of the inner radiation belt to the violent Sun-Earth connection events of October–November 2003, *Geophys. Res. Lett.*, *32*, L03S06, doi:10.1029/2004GL021502.

Lorentzen, K. R., J. E. Mazur, M. D. Looper, J. F. Fennell, and J. B. Blake (2002), Multisatellite observations of MeV ion injections during storms, *J. Geophys. Res.*, *107*(A9), 1231, doi:10.1029/2001JA000276.

Press, W. H., B. P. Flannery, S. A. Teukolsky, and W. T. Vetterling (2007), *Numerical Recipes: The Art of Scientific Computing*, 3rd ed., Cambridge Univ. Press, New York, isbn:978-0-521-88068-8.

Selesnick, R. S., M. K. Hudson, and B. T. Kress (2010), Injection and loss of inner radiation belt protons during solar proton events and magnetic storms, *J. Geophys. Res.*, *115*, A08211, doi:10.1029/2010JA015247.

Sergeev, V. A., and N. A. Tsyganenko (1982), Energetic particle losses and trapping boundaries as deduced from calculations with a realistic magnetic-field model, *Planet. Space Sci.*, *30*(10), 999–1006.

Speiser, T. Q. (1965), Particle trajectories in model current sheets: 1. Analytical solutions, *J. Geophys. Res.*, *70*, 4219–4226, doi:10.1029/JZ070i017p04219.

Taylor, H. E., and R. J. Hastie (1971), Nonadiabatic behavior of radiation-belt particles, *Cosmic Electrodyn.*, *2*, 211–223.

Tsyganenko, N. A. (1989), A magnetospheric magnetic field model with a warped tail current sheet, *Planet. Space Sci.*, *37*, 5–20.

Tu, W., G. S. Cunningham, Y. Chen, M. G. Henderson, E. Camporeale, and G. D. Reeves (2013), Modeling radiation belt electron dynamics during GEM challenge intervals with the DREAM3D diffusion model, *J. Geophys. Res. Space Physics*, *118*, 6197–6211, doi:10.1002/jgra.50560.

West, H. I., R. M. Buck, and M. G. Kivelson (1978), On the configuration of the magnetotail near midnight during quiet and weakly disturbed periods: Magnetic field modeling, *J. Geophys. Res.*, *83*, 3819–3829, doi:10.1029/JA083iA08p03819.

Young, S. L., R. E. Denton, B. J. Anderson, and M. K. Hudson (2002), Empirical model for μ scattering caused by field line curvature in a realistic magnetosphere, *J. Geophys. Res.*, *107*(A6), 1069, doi:10.1029/2000JA000294.

Young, S. L., R. E. Denton, B. J. Anderson, and M. K. Hudson (2008), Magnetic field line curvature induced pitch angle diffusion in the inner magnetosphere, *J. Geophys. Res.*, *113*, A03210, doi:10.1029/2006JA012133.

Zou, H., Q. G. Zong, G. K. Parks, Z. Y. Pu, H. F. Chen, and L. Xie (2011), Response of high-energy protons of the inner radiation belt to large magnetic storms, *J. Geophys. Res.*, *116*, A10229, doi:10.1029/2011JA016733.